

## Intensities of Low-Energy-Electron-Diffraction Beams from Be(0001)

F. Jona,\* J. A. Strozier, Jr.,\* and J. Kumar\*  
*State University of New York, Stony Brook, New York 11790*

and

R. O. Jones  
*Institut für Festkörperforschung der Kernforschungsanlage, Jülich, 517 Jülich, Germany*  
 (Received 24 January 1972)

The intensities of several low-energy-electron-diffraction (LEED) beams from a clean Be(0001) surface are measured as functions of incident-electron energy, azimuth, and angle of incidence. The resulting LEED spectra (intensities vs energy) of the specular and of two nonspecular beams are plotted for two different azimuth angles from 20 to 300 eV and every 2° in incident angle from 0° to 24°. Several of the nonspecular spectra are compared with the results of calculations done by means of a band-matching perturbation approach utilizing a suitable pseudopotential. The comparison shows encouraging agreement considering, in particular, the speed and simplicity of the computations. Attention is drawn to the fact that the intensities of nonspecular beams from the basal plane of the hexagonal-close-packed lattice depend on the way in which the structure is terminated at the surface, in contrast to the close-packed {111} face of the face-centered-cubic lattice, for which termination plays no role.

### I. INTRODUCTION

The chief problem in the process of low-energy-electron diffraction (LEED) is to establish a unique and reversible relationship between the structure of the scattering surface layer and the intensities of the scattered electrons. These intensities are, of course, functions of the reciprocal-lattice vectors, of energy, and of the incident angles. The correct solution of the LEED problem must therefore be able to explain the intensities of all observable beams at all energies and all possible incident angles, not only for one but eventually for any surface of a given material. Owing to the pronounced dynamical (as contrasted to kinematical) character of the diffraction of low-energy electrons, any theory capable of providing a solution, even approximate, to the LEED problem is by necessity complicated. The calculations of the diffraction spectra expected from a given surface are lengthy and hence costly because of their demand on computer time. For these reasons, a considerable number of theoretical treatments of the LEED problem have been proposed recently,<sup>1-21</sup> but few have been applied to complete calculations of theoretical LEED spectra for specific surfaces. There is, on the other hand, a limited choice of reasonably reliable experimental data with which to test the calculated LEED spectra. The collection of such data from atomically clean surfaces over a wide range of energies and incident angles is tedious and time-consuming work. So far, only one body of data that may be called a fairly complete set has been published in the literature: This involves three surfaces of aluminum (Al{001}, Al{111}, and Al{110}).<sup>22</sup> Somewhat less complete

sets are available for silver (Ag{111}<sup>23,23a</sup> and, with provisory character, Ag{001}<sup>24</sup>) and for copper (Cu{001}<sup>25</sup> and Cu{111}<sup>26</sup>). It is coincidental that all three of these materials have the face-centered-cubic structure.

Because of the encouraging agreement between calculated and observed LEED spectra<sup>4,5,9,12,13,18,20,27</sup> it is interesting to examine surfaces of some other, non-fcc material. An excellent candidate for such scrutiny is beryllium, for a variety of reasons: It is moderately hard and refractory, and thus can be polished and cleaned sufficiently well for quantitative LEED investigations; it has a very high Debye temperature (1160°K) and should thus produce relatively little thermal diffuse scattering at room temperature; it is the lightest element that crystallizes with the hexagonal-close-packed structure and its electronic band structure is reasonably well known. In addition, an independent and contemporary study of cleaved beryllium surfaces by means of LEED, carried out by Baker and Blakely,<sup>28</sup> can provide a useful and reliable check of data collected from clean but not cleaved surfaces.

The present paper has thus a dual purpose. First, it presents a reasonably complete set of experimental LEED spectra from the Be(0001) surface and compares it critically with the set collected by Baker and Blakely.<sup>28</sup> Second, it presents results of calculations of nonspecular-beam intensities which were carried out with a computationally simple computer program.<sup>27</sup> Comparison of the calculated with the observed LEED spectra from Be(0001) shows satisfactory agreement over a wide range of energies and incident angles, thus confirming and completing a recent study of the specular beam's intensities from the same surface.<sup>19</sup>

## II. EXPERIMENTAL PROCEDURES

### A. Sample Preparation

The starting material was a single crystal of beryllium with bulk purity 99.95%. Platelets approximately 0.060 in. thick were cut from this single crystal by means of a wire saw with silicon-carbide abrasive, the orientation being such that the major surfaces of the platelets were roughly perpendicular to the hexagonal  $c$  axis, i. e., parallel to the basal plane of the hexagonal-close-packed lattice. The orientation was then corrected by means of a polishing wheel with, successively, 325-, 400-, and 600-grit paper to be within  $1^\circ$ - $4^\circ$  off the basal plane. Backreflection Laue diffraction patterns were used to check the orientation of the sample during all preparation procedures. The final steps in these procedures consisted of lapping the major surfaces of the platelets with 1900-grit powder (thereby improving the orientation with respect to the basal plane and reducing the thickness to about 0.020 in.); and finally, polishing with 0.05- $\mu\text{m}$  alumina powder. The final sample was a rectangular platelet  $\frac{5}{8}$  in. in length,  $\frac{1}{4}$  in. in width, and 0.020 in. in thickness, the major surfaces being parallel to the (0001) plane of the hexagonal-close-packed lattice to within  $0.5^\circ$ . These surfaces were then electropolished on a rotating wheel with a solution of 100-cm<sup>3</sup> H<sub>3</sub>PO<sub>4</sub>, 30-cm<sup>3</sup> H<sub>2</sub>SO<sub>4</sub>, 30-cm<sup>3</sup> glycerin, and 30-cm<sup>3</sup> ethyl alcohol, and a current of 3 A at 50 V for 2 min. The amount of material removed during the electropolishing treatment corresponded to a reduction in thickness of about 0.001 in.

### B. Surface Cleaning

The sample was mounted on a special holder, described elsewhere,<sup>29</sup> which allows rotation of the surface to be studied around two mutually perpendicular directions, and then introduced into the LEED system. This was a conventional display-type system with three grids and a fluorescent screen.<sup>30</sup> *In situ* cleaning of the surface was started after attainment of a base pressure of about  $1 \times 10^{-10}$  torr. Earlier investigations by Adams<sup>31</sup> showed that high-contrast LEED patterns of a Be(0001) surface could be observed after either (i) heating to 1000°C for 5 min, or (ii) argon-ion bombardment at  $(1-5) \times 10^{-2}$  torr and 1000 V for 30 min, followed by annealing at 750°C for 30 min. Since the vapor pressure of beryllium is approximately  $10^{-3}$  torr at 1000°C it is expected (and it was in fact observed<sup>31</sup>) that the surface would be thermally etched during the high-temperature-cleaning treatment. Adams reported, in fact, that a series of such treatments deteriorated the surface, and hence the LEED pattern, to such an extent that the intensities of the diffracted beams

could not be reproduced from treatment to treatment. For this reason, we decided to avoid this particular procedure for surface cleaning and concentrate instead on a sequence of argon-ion bombardments and anneals.

The maximum convenient pressure of argon in our system (convenient in the sense that the sputter-ion pump alone is sufficient, without the help of forevacuum pumps, to reestablish ultra-high vacuum conditions after each ion bombardment) is in the low  $10^{-4}$ -torr range. For this reason, our ion-bombardment treatments were carried out, typically, at pressures of  $(1-2) \times 10^{-4}$  torr of argon, with ion energies of the order of 600 V and ion currents of the order of  $2 \mu\text{A}/\text{cm}^2$ . Each treatment lasted 1-2 h and was followed by an anneal of  $\frac{1}{2}$ -1 h at approximately 750°C. The procedure was repeated for a total bombardment time of about 20 h, although acceptable LEED patterns were observed after a total of about 15 h.

Observation of the LEED pattern and subjective evaluation of its high-contrast quality were the only criteria used for surface cleanliness. This is unfortunate (Auger-electron spectroscopy was not available to us at the time) because we cannot exclude with certainty the possible presence of minute amounts of oxygen on the surface during collection of intensity data. For the following reasons, however, we believe that the data reported below represent a valid set: (a) Spot checks done at different times over a period of several months showed that the LEED spectra were always reproduced very satisfactorily. (b) Controlled adsorption of oxygen on Be(0001), as shown by Baker and Blakely,<sup>29</sup> and confirmed by us, causes a general decrease in intensity of the LEED beams concomitant with an over-all increase in background intensity, but no shifts in energy of the LEED spectra and no appearance of extra beams. The oxygen atoms are disordered on Be(0001). (c) Our intensity data reproduce Baker and Blakely's data (obtained from a cleaved surface) fairly well (see discussion below), but are more complete regarding nonspecular beams and azimuthal dependence of the specular beam.

### C. Collection of Intensity Data

The intensities of the diffracted beams were measured by monitoring the brightnesses of the corresponding LEED spots on the fluorescent screen with a suitable spot photometer.<sup>32</sup> In general, the procedures adopted in this experimental work were the same as described in an earlier publication.<sup>22</sup> These procedures involved the plotting of the LEED spectra on an X-Y recorder; the determination of the current incident upon the sample; the compensation of earth's and stray magnetic fields; the determination of normal incidence; the calibration

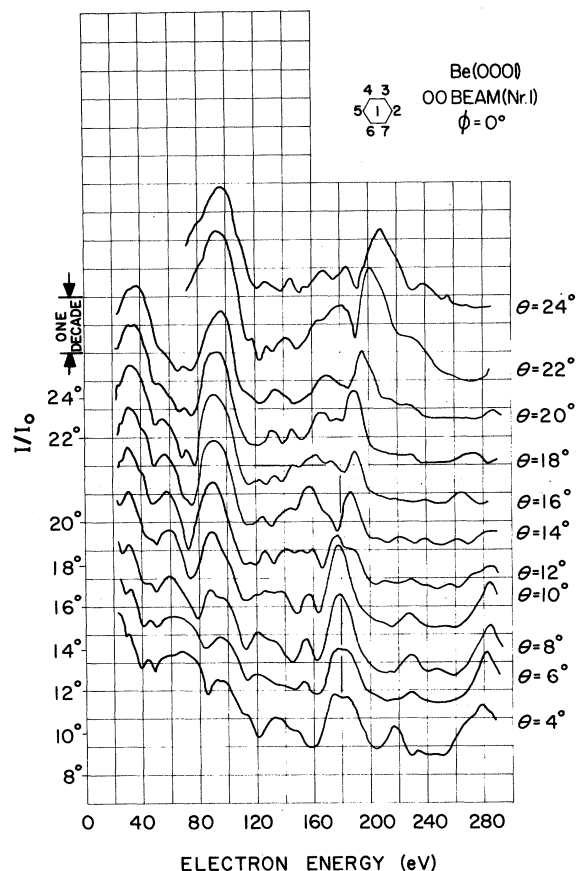


FIG. 1. Be(0001). Experimental angular dependence of the 00 spectrum:  $\theta$  varies from  $4^\circ$  to  $24^\circ$  while  $\phi$  is fixed at  $\phi = 0^\circ$ . The curves have been translated in the vertical direction by different amounts to avoid overlap. The numbers on the left-hand side indicate the levels at which the scales pertaining to the curves with the corresponding  $\theta$  angles have the same (arbitrary) value. Thus, any two spectra for different values of  $\theta$  can be compared quantitatively with one another by translating the corresponding curves until the tickmarks with the corresponding  $\theta$  values coincide. The tickmarks for  $6^\circ$  and  $4^\circ$  are located  $\frac{3}{4}$  of a decade and  $1\frac{1}{2}$  decade below the  $8^\circ$  tickmark, respectively.

of the azimuthal angle; and the application of a biasing voltage between the sample and the first grid in the LEED optics. A novel procedure was introduced for recording and normalizing the intensity-vs-energy curves: The raw data were fed, during the measurements, into a time-shared on-line computer. The output of the spot photometer (after suitable amplification) and the electron-beam voltage (after suitable deamplification) were transmitted to the computer via telephone lines over a distance of about 4 mi. The data were digitized, tested for internal consistency, and then stored on cards at the computer end. Normalization of the data (carried out by dividing each value

$I$  of the intensity by the value  $I_0$  of the electron current incident on the surface at the same energy), and plotting of the LEED spectra on linear or logarithmic scales were done subsequently whenever needed.

Since the fluorescent screen that is part of the LEED optics subtends an angle of only about  $100^\circ$  at the sample, the nonspecular beams are not visible on the screen at very low voltages, under field-free conditions. To make them visible on the screen it is necessary to bias the first grid positively with respect to the sample. The intensity data of nonspecular beams were therefore collected in two steps. First, the data were collected, under field-free conditions, from 300 V down to the voltage at which the corresponding diffraction spot moved off the fluorescent screen. Second, the data were taken again, after application of a suitable bias voltage between first grid and sample (typically about 150 V) from approximately 120 V down to the emergence voltage of the corresponding beam. Subsequently, both sets of data were separately normalized [the normalizing curves  $I_0(V)$  are different in the two cases] and finally matched to one another by bringing into coincidence the overlapping portions of the spectra. The result is thus a single spectrum, for each beam measured, extending from emergence to about 300 V.

The measured spectra are plotted on a logarithmic scale in Figs. 1-7. Three beams (the specular and two nonspecular beams) are reported for each of two values of the azimuth angle  $\phi$ , namely,  $\phi = 0^\circ$  and  $\phi = 30^\circ$ . The meaning of these azimuthal positions is clarified by the hexagons sketched on top of each figure. The hexagons represent, schematically, the LEED patterns observed, the diffraction spots being located at the center (specular beam labeled No. 1) and at the corners of the hexagons (nonspecular beams, labeled from No. 2 to No. 7). At constant azimuth  $\phi$ , the incident angle  $\theta$  is varied by assuming that the incident electron beam is fixed and perpendicular to the plane of the drawing, while the sample is rotated. The angle of incidence  $\theta$  is defined as the angle formed by the incident electron beam with the normal to the sample surface. The rotation of the latter is assumed to occur horizontally, moving the specular spot to the right for increasing angle  $\theta$ . In Figs. 1-6, the angle  $\theta$  varies from  $4^\circ$  for the specular beam, and from  $0^\circ$  for the nonspecular beams, up to  $24^\circ$  in steps of  $2^\circ$ . In Fig. 7, the angle  $\theta$  was held fixed (at  $14^\circ$ ) and the azimuthal angle  $\phi$  was varied from  $0^\circ$  to  $30^\circ$  in steps of  $5^\circ$ .

All data were taken at room temperature. The estimated accuracy of the energy scale is  $\pm 2$  eV. No correction was applied for the difference in contact potential between the sample and the cathode of the electron gun. The angles quoted in the figures are estimated to be accurate to within  $\pm 2^\circ$ .

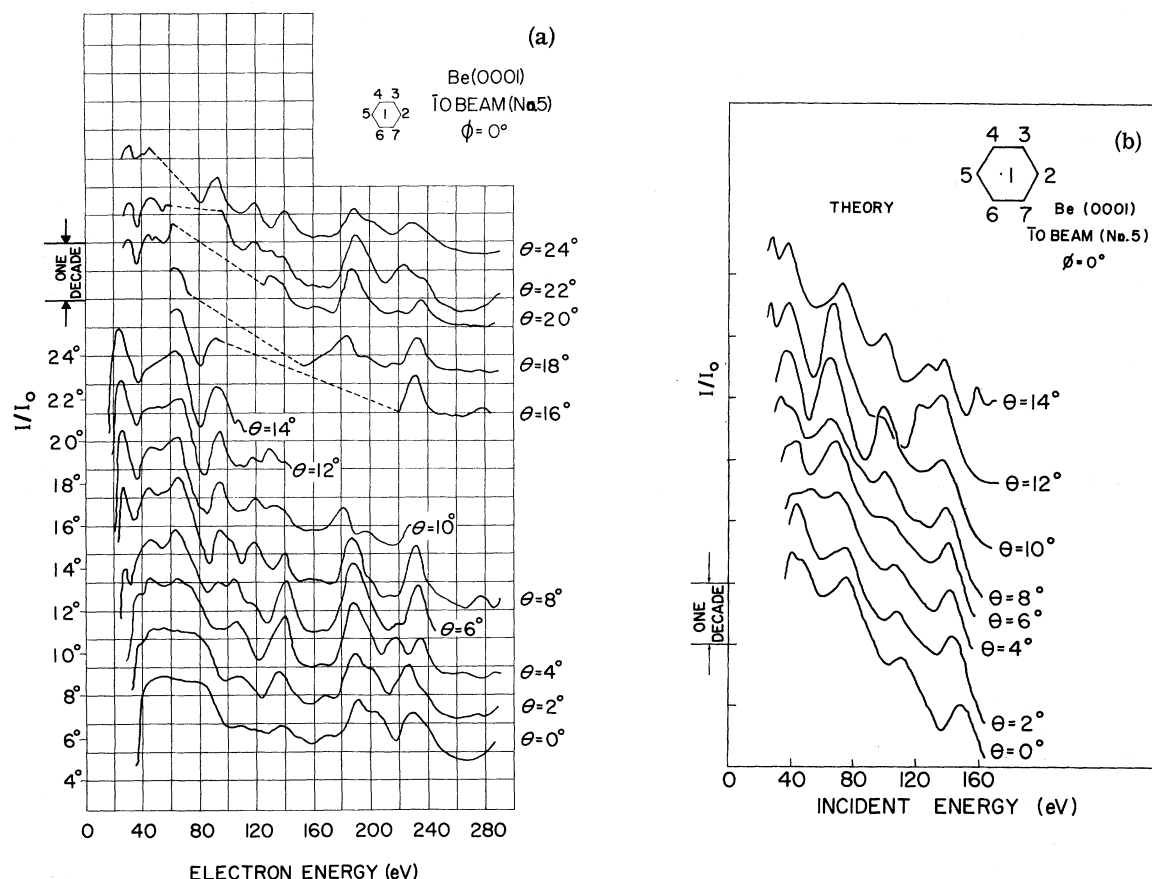


FIG. 2. (a) Be(0001). Experimental angular dependence of the  $\bar{1}0$  spectrum (spot No. 5 on schematic LEED pattern shown on top):  $\theta$  varies from  $0^\circ$  to  $24^\circ$ , while  $\phi$  is fixed at  $\phi = 0^\circ$ . The spectra have been displaced vertically as described in the caption to Fig. 1. The tickmarks for  $2^\circ$  and  $0^\circ$  are located  $\frac{3}{4}$  of a decade and  $1\frac{1}{2}$  decade below the  $4^\circ$  tickmark. The spectra for  $\theta = 10^\circ$  through  $\theta = 24^\circ$  are not complete (dotted lines) because the corresponding diffraction spots were occluded by the drift tube of the electron gun. (b) Calculated angular dependence of the  $\bar{1}0$  spectrum for  $\phi = 0^\circ$ .

above 40–50 eV (although the relative accuracy may be  $\pm 0.5^\circ$ ). Below this energy, the accuracy of the values of  $\theta$  and  $\phi$  is probably rather worse, although difficult to estimate, owing to our inability to eliminate completely the residual local magnetic and electrostatic fields.

#### D. Comparison with Other Data

Although Adams<sup>31</sup> was the first to report LEED observations of beryllium surfaces, at the time of writing only Baker and Blakely<sup>28</sup> have collected a fairly complete set of intensity data from Be(0001). Baker and Blakely's set consists of the angular dependence of the 00 beam for  $\phi = 0^\circ$  and  $\phi = 30^\circ$  (similar to our Figs. 1 and 4), and of the two non-specular spectra at  $\theta = 5^\circ$  and  $\phi = 30^\circ$ . cursory inspection of Baker and Blakely's set and of ours indicates satisfactory agreement within the quoted experimental accuracies. We have, however, made

a careful curve-by-curve comparison of the two sets of data<sup>33</sup> by directly overlaying one on top of the other.

The results of this comparison were the following: All the spectra in Fig. 1 (angular dependence of 00 beam for  $\phi = 0^\circ$ ) are displaced on the average by  $(5 \pm 2)$  eV toward higher energies with respect to the corresponding figure of Baker and Blakely. A curve-by-curve comparison cannot be done rigorously because the  $\theta$  angles quoted are never exactly the same in the two figures. However, for  $\theta < 8^\circ$  there is good correspondence of the  $\theta$  values; for  $\theta > 8^\circ$ , the  $\theta$  values quoted by us are consistently  $1^\circ$ – $2^\circ$  lower than the  $\theta$  values quoted by Baker and Blakely for the "same" curve. The general agreement of peak positions, peak shapes, and general intensities is fair to good. There is, however, one shoulder peak around 100 eV in Baker and Blakely's data that never develops fully in our set of Fig. 1.

This general trend is repeated for the data in Fig. 4. Note that the curves in the corresponding figure of Baker and Blakely were not normalized, although this should not affect the peak positions too much. Our energy scale is on the average  $(6 \pm 2)$  eV higher than Baker and Blakely's. The  $\theta$  values correspond well for  $\theta < 8^\circ$ , while for  $\theta > 8^\circ$  there is a difference of about  $2^\circ$  (our values being lower than Baker and Blakely's). The general correspondence of peaks is good. As for the nonspecular beams, only one spectrum (Baker and Blakely's  $\bar{1}\bar{1}$  at  $\theta = 5^\circ$  versus our beam No. 4 at  $\theta = 4^\circ$  or  $6^\circ$ ) is common to both sets, and for this the correspondence is good.

Two main points arise from this detailed comparison with Baker and Blakely's data: (i) There is a difference of approximately 6 eV, on the average, between the two sets of data; (ii) there is a difference of approximately  $2^\circ$ , on the average, between any two  $\theta$  values quoted for the "same" spectrum. These differences are indicative of a systematic error, because they always have the

same sign. Discrepancy (i) is reduced by the fact that Baker and Blakely have corrected their energy scale for the contact-potential difference between sample and cathode (the correction being<sup>28</sup> - 3.5 V), whereas we have not. So, the average discrepancy is reduced from 6 to 2.5 eV if we assume, as is likely, that the same contact-potential correction would apply to our data as well. This difference, although due to a systematic error of unknown origin, is overlapped in part by the uncertainties (of  $\pm 2$  eV) quoted by both Baker and Blakely<sup>28</sup> and by us. As for the difference of  $2^\circ$  in the  $\theta$  values this also just barely lies within the quoted experimental accuracies (of  $\pm 2^\circ$ ). We conclude, therefore, that, by and large, the agreement between Baker and Blakely's set of data and that part of our own set which overlaps it is satisfactory within the quoted experimental uncertainties. The lack, in our data, of the shoulder peak exhibited by Baker and Blakely's set for the 00 beam at  $\phi = 0^\circ$  and about 100 eV we ascribe to a possible contami-

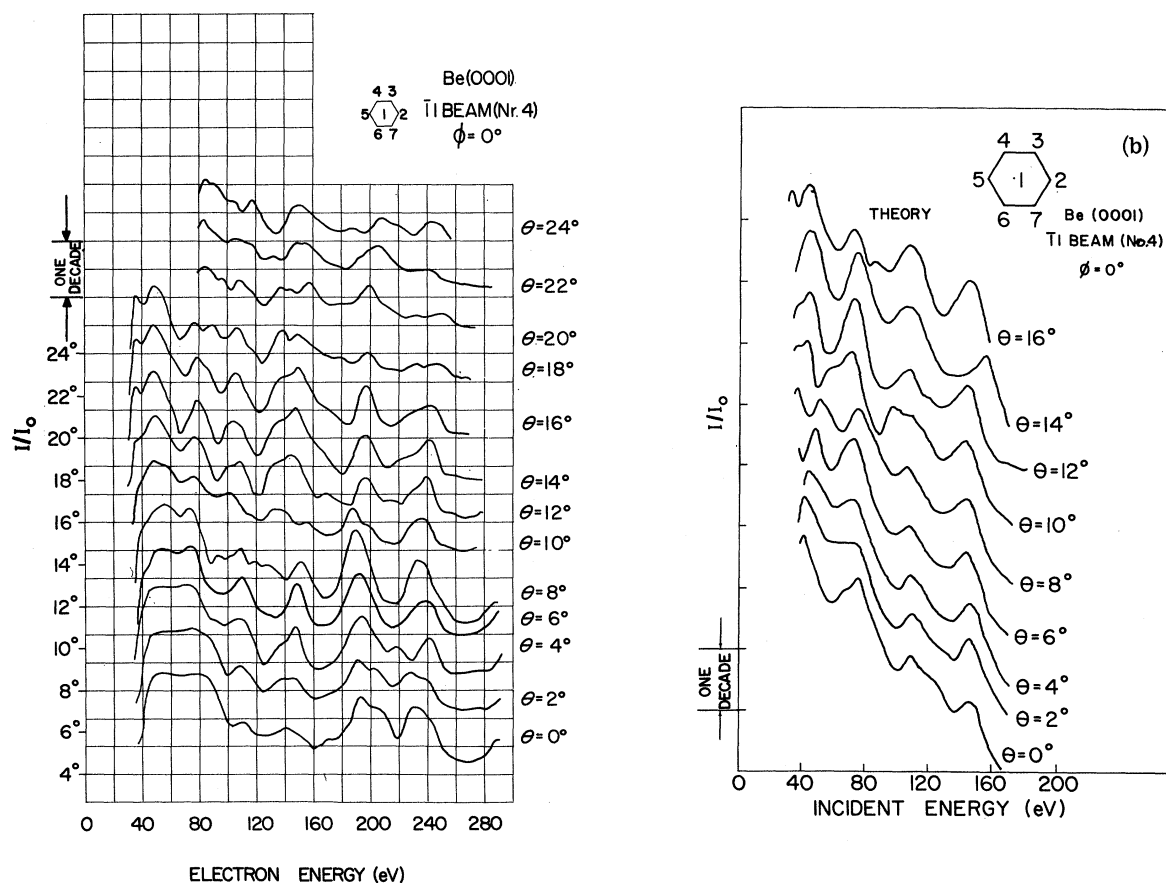


FIG. 3. (a) Be(0001). Experimental angular dependence of the  $\bar{1}\bar{1}$  spectrum (spot No. 4 on schematic LEED pattern shown on top):  $\theta$  varies from  $0^\circ$  to  $24^\circ$ , while  $\phi$  is fixed at  $\phi = 0^\circ$ . The spectra have been displaced vertically as described in the caption to Fig. 1. (b) Calculated angular dependence of  $\bar{1}\bar{1}$  spectrum for  $\phi = 0^\circ$ .

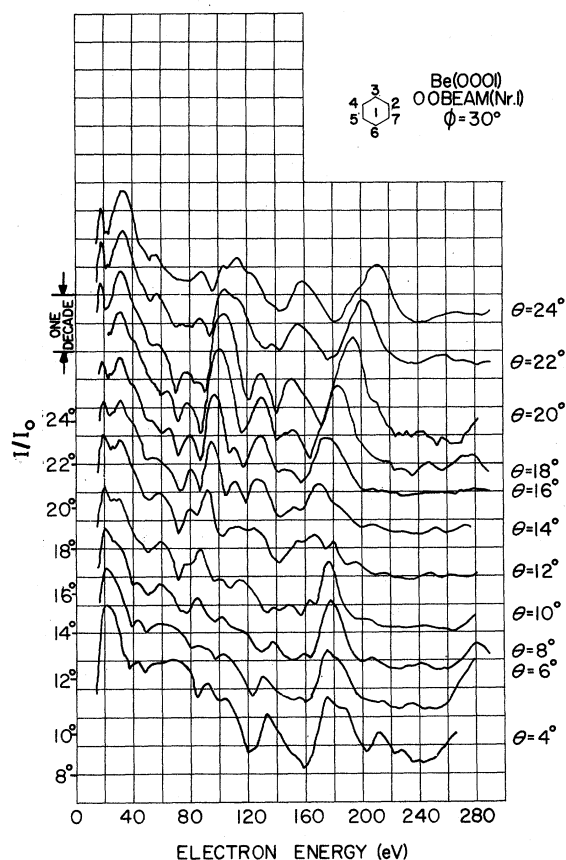


FIG. 4. Be(0001). Experimental angular dependence of the 00 spectrum:  $\theta$  varies from  $4^\circ$  to  $24^\circ$ , while  $\phi$  is fixed at  $\phi = 30^\circ$ . The spectra have been displaced vertically as described in the caption to Fig. 1.

nation of our surfaces during this particular measurement. It should be noted that, while our data were collected with the sample at room temperature, Baker and Blakely collected theirs with the sample at liquid-nitrogen temperature. However, since the Debye temperature of beryllium is very high ( $1160^\circ\text{K}$ ) one would not expect much difference between LEED spectra taken at room temperature and those taken at liquid-nitrogen temperature. Considering that our surfaces were cleaned by ion bombardments, while Baker and Blakely's were cleaned *in situ*, we conclude that the general agreement discussed above is further confirmation of the efficiency of the ion-bombardment cleaning method for achieving clean surfaces in ultrahigh vacuum.

### III. CALCULATIONS AND COMPARISON WITH EXPERIMENT

In earlier papers,<sup>19</sup> several LEED spectra of the specular beam from the basal plane of beryllium were calculated by means of a band-matching perturbation approach. This approach was justified because for energies above the threshold for plas-

mon creation (approximately 20 V), and for materials with weak scattering pseudopotentials, the strength of the inelastic scattering promotes rapid convergence of the expansion in Bloch states. Particular advantages of this method are its applicability to arbitrary angles of incidence and the speed of computation of several points per second on the IBM 360-67 machine, even with a detailed energy-dependent nonlocal pseudopotential. The spectra calculated with this band-matching procedure were compared with the experimental curves of Baker and Blakely<sup>28</sup> and encouraging agreement was found over a wide range of incident energies and angles.

To examine the wider applicability of the method, we include here calculated spectra for several nonspecular beams. In particular the intensities of the  $\bar{1}0$  and  $\bar{1}1$  beams for  $\phi = 0^\circ$  are computed for several values of the energy and of the incident angle  $\theta$  and compared with experiment. The procedure followed for the calculation of the potential and of the LEED intensities is the same as pre-

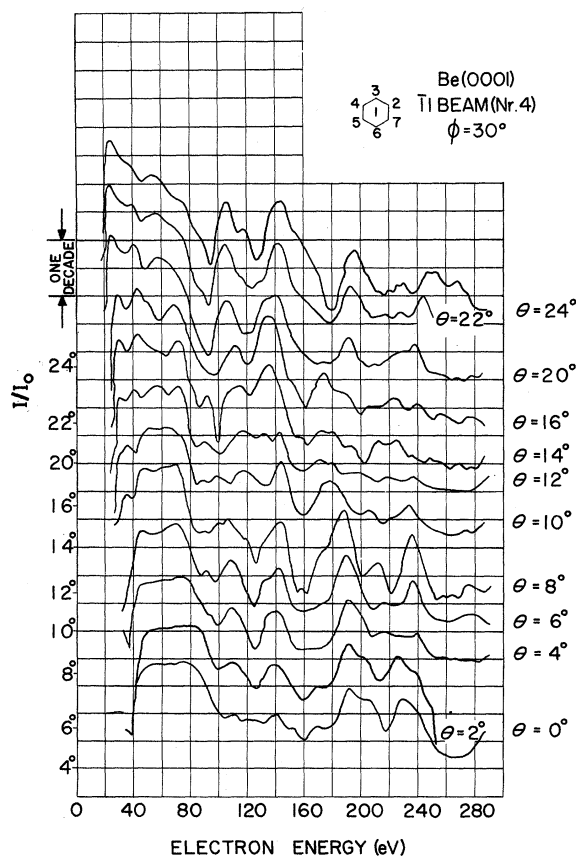


FIG. 5. Be(0001). Experimental angular dependence of the  $\bar{1}1$  spectrum (spot No. 4 on schematic LEED pattern shown on top):  $\theta$  varies from  $0^\circ$  to  $24^\circ$ , while  $\phi$  is fixed at  $\phi = 30^\circ$ . The spectra have been displaced vertically as described in the caption to Fig. 1.

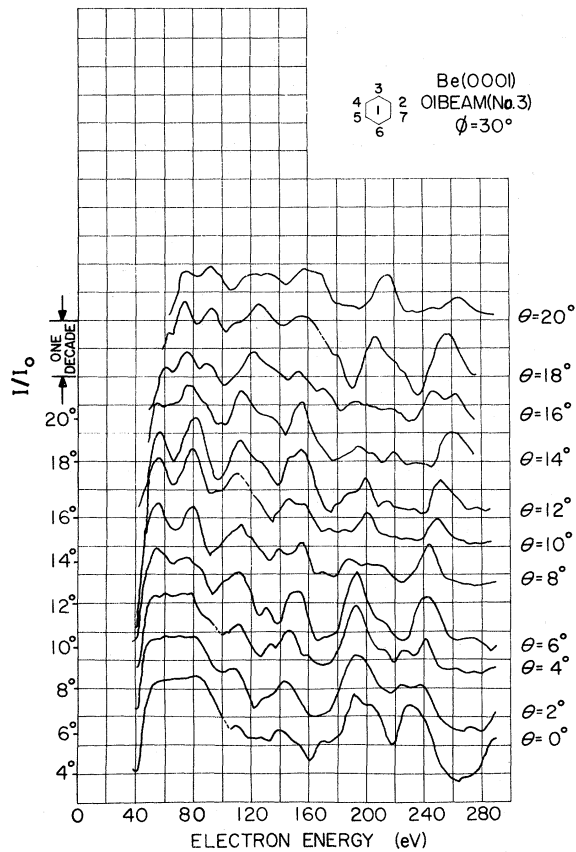


FIG. 6. Be(0001). Experimental angular dependence of the 01 spectrum (spot No. 3 on schematic LEED pattern shown on top):  $\theta$  varies from  $0^\circ$  to  $24^\circ$ , while  $\phi$  is fixed at  $\phi = 30^\circ$ . The spectra have been displaced vertically as described in the caption to Fig. 1.

viously reported.<sup>19</sup> The results are shown in Figs. 2(b), 3(b), and 8. Over-all agreement in peak position and structure is at least as good as reported earlier for the specular beams. The arbitrary, although physically reasonable, elimination of the potential step at the interface in the specular-beam calculation is unnecessary here as the reflection due to the discontinuity is specular and hence does not interfere with the nonspecular beams. This can be seen formally by inspection of the expressions for the amplitudes of the specular and any nonspecular beam.

One interesting point arises from the two different ways in which the hexagonal-close-packed basal plane can terminate at the surface. The hexagonal lattice is comprised of layers with the well-known stacking sequence  $ABAB\cdots$ . Termination of the crystal midway between planes  $A$  and  $B$  will yield, in general, different LEED spectra for the nonspecular beams from termination midway between planes  $B$  and  $A$ . This is due to inelastic effects which effectively give a greater weight to diffraction from the first layer and successively

less weight to diffraction from succeeding layers. The specular beam is not affected, because the reciprocity theorem<sup>34</sup> guarantees its invariance to the order of termination. The differences in the intensities of the nonspecular beams for different terminations, however, are considerable and can be illustrated by a simple kinematic calculation in which absorption is included.

#### A. Kinematic Calculation

We fix the  $z$  axis such that the surface lies in the  $xy$  plane. The attenuation of the beam into the crystal by inelastic scattering relaxes the diffraction condition in the  $z$  direction. Thus the intensity of a diffracted beam with scattering vector  $\vec{K} = \vec{k}' - \vec{k}$  is proportional to<sup>35</sup>

$$I(\vec{K}) \propto \delta(\vec{K}'' - \vec{g}'') |L(K^z)|^2 |S(\vec{K})|^2, \quad (1)$$

where  $L(\vec{K}) \equiv \sum_i \exp(-i\vec{K}^z \cdot \vec{R}_i)$  and the structure factor term  $S(\vec{K}) \equiv \sum_j e^{-i\vec{K} \cdot \vec{r}_j}$ . Here  $\vec{k}'$  and  $\vec{k}$  are the wave vectors of the incident and diffracted beams;  $K''$  and  $\vec{g}''$  are the components of  $\vec{K}$  and  $\vec{g}$  parallel to the surface.  $\vec{g}$  being a reciprocal-lattice vector:

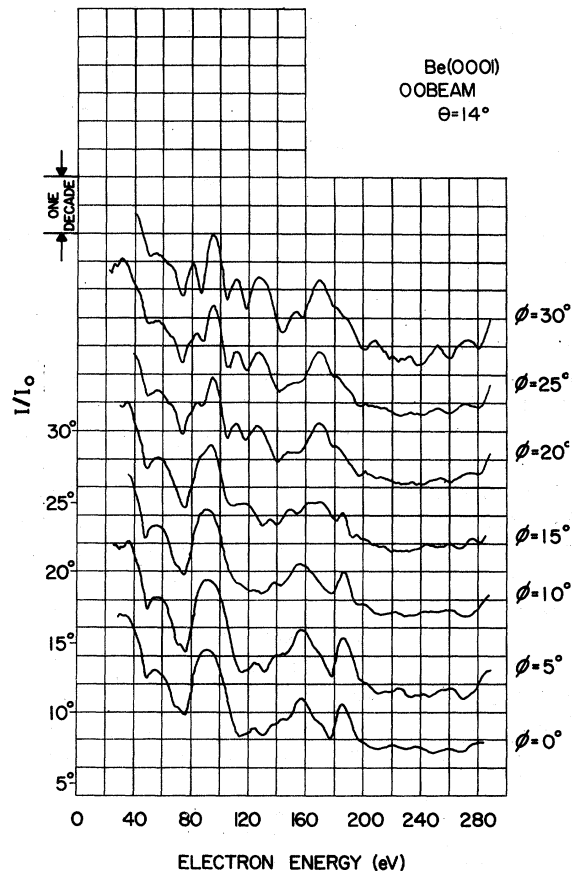


FIG. 7. Be(0001). Experimental dependence of the 00 spectrum upon azimuth angle  $\phi$  for constant incident angle  $\theta = 14^\circ$ . The spectra have been displaced vertically as described in the caption to Fig. 1.

$K^\perp$  is the component of  $\vec{K}$  perpendicular to the surface;  $\vec{R}_l$  is the lattice vector to the origin of the  $l$ th unit cell; and  $\vec{r}_j$  is the vector from the origin of the unit cell to the  $j$ th atom in the unit cell. The Kronecker  $\delta(\vec{K}'' - \vec{g}'')$  is a consequence of the two-dimensional periodicity everywhere. For simplicity we consider the incident beam normal to the surface. Conservation of energy and the factor  $\delta(\vec{K}'' - \vec{g}'')$  yield the following expression for the backward-scattered beams:

$$\vec{K} = \vec{K}'' + \vec{K}^\perp, \quad \vec{K}'' = \vec{g}'' = g_x \hat{i} + g_y \hat{j},$$

$$\vec{K}^\perp = \{ (E + V_0)^{1/2} + [E + V_0 - (g'')^2]^{1/2} \} \hat{k},$$

where  $\hat{i}$ ,  $\hat{j}$ , and  $\hat{k}$  are unit vectors in the directions  $x$ ,  $y$ , and  $z$ , respectively,  $E$  is the incident-beam energy, and  $V_0$  is the inner potential. Inelastic effects are simulated by an imaginary component of  $V_0$ . Thus  $K^\perp$  is complex with

$$\vec{K}^\perp = (k + ik') \hat{k}.$$

The distinction between terminations (either  $A$  or  $B$ ) can be expressed as a difference in the third factor of Eq. (1), the structure factor  $S(\vec{K})$ . The second factor is independent of termination and is easily evaluated to be

$$|L(K^\perp)|^2 = \frac{1}{1 + e^{-2k'c} - 2e^{-k'c} \cos kc}, \quad (2)$$

where  $c$  is the lattice parameter along the sixfold axis of the hexagonal unit cell. This expression yields the usual Bragg peaks, lifetime broadened by inelastic scattering.

Let us now focus our attention on the structure factor, which for the hexagonal-close-packed structure is the sum of two terms  $S = e^{-i\vec{K} \cdot \vec{r}_1} + e^{-i\vec{K} \cdot \vec{r}_2}$ . The basis vectors of the hexagonal lattice can be taken as (see Fig. 10)

$$\vec{a} = \frac{1}{2}\sqrt{3} a \hat{i} + \frac{1}{2} a \hat{j}, \quad \vec{b} = -a \hat{j}.$$

Then the basis vectors of the reciprocal lattice are given by

$$\vec{a}^* = \frac{2}{\sqrt{3}} \frac{1}{a} \hat{i} \quad \text{and} \quad \vec{b}^* = + \frac{1}{\sqrt{3}} \frac{1}{a} \hat{i} - \frac{1}{a} \hat{j}.$$

Each of the two terminations gives rise to a different set of  $\vec{r}_j$  vectors in the unit cell. From Fig. 10 we see that the  $\vec{r}_j$ 's for termination "A" are

$$\vec{r}_{A,1} = 0, \quad \vec{r}_{A,2} = \frac{1}{3}\sqrt{3} a \hat{i} + \frac{1}{2} c \hat{k};$$

and for termination "B,"

$$\vec{r}_{B,1} = 0, \quad \vec{r}_{B,2} = \frac{1}{6}\sqrt{3} a \hat{i} - \frac{1}{2} a \hat{j} + \frac{1}{2} c \hat{k}.$$

If we consider a general diffracted beam given by

$$\vec{K}'' = 2\pi n \vec{a}^* + 2\pi m \vec{b}^* \quad \text{and} \quad \vec{K}^\perp = (k + ik') \hat{k},$$

where  $n$  and  $m$  are integers, then it is easy to

show that the absolute squares of the structure factors for the two different terminations are

$$|S_A|^2 = 1 + e^{-k'c} + 2e^{-k'c/2} \cos\left[\frac{2}{3}\pi(2n+m) - \frac{1}{2}kc\right],$$

$$|S_B|^2 = 1 + e^{-k'c} + 2e^{-k'c/2} \cos\left[\frac{2}{3}\pi(n+2m) - \frac{1}{2}kc\right]. \quad (3)$$

While generally  $|S_A| \neq |S_B|$ , there are important special cases in which they are equal and termination is therefore of no importance. These are (a) when  $2n+m$  is a multiple of three ( $n=m$  is a special case). It follows immediately that  $n+2m$  is also a multiple of three, and hence the arguments of the cosines in Eq. (3) are identical (with-in modulo  $2\pi$ ). (b) The second case is when there is a "Bragg" reflection; i. e., when  $|L(K^\perp)|$  [Eq. (2)] is a maximum. This occurs for  $-kc = 2\pi l$ ,  $l = \text{integer}$ ; and follows at once from the identity

$$\cos\left[\frac{2}{3}\pi(2n+m) + \pi l\right] = \cos\left[\frac{2}{3}\pi(n+2m) + \pi l\right]$$

for any set of integers  $n, m, l$ . (c) The third case is when there is no absorption; i. e., when  $k'c = 0$ . Then  $\delta(\vec{K}'' - \vec{g}'') |L(K^\perp)|^2$  is proportional to  $\delta(\vec{K}'' - \vec{g}'')$  which yields a nonzero contribution only at a Bragg reflection; in which case point (b) above applies.

In all other cases, Eq. (3) gives differences for the two terminations. For example, if we calculate the intensities halfway between the "Bragg" reflections, we have  $kc = \pi l$ ,  $l$  being an odd integer. Then the differences  $|S_A|^2 - |S_B|^2$  are given by  $2\sqrt{3} e^{-k'c/2} C_{n,m}$ , where the quantities  $C_{n,m}$  for  $l=1, 5, 9, \dots$  are given by

$$C_{n,m} = 1 \quad \text{if } n-m = 1, 4, 7, \dots \text{ or } -2, -5, -8, \dots;$$

$$C_{n,m} = -1 \quad \text{if } n-m = 2, 5, 8, \dots \text{ or } -1, -4, -7, \dots$$

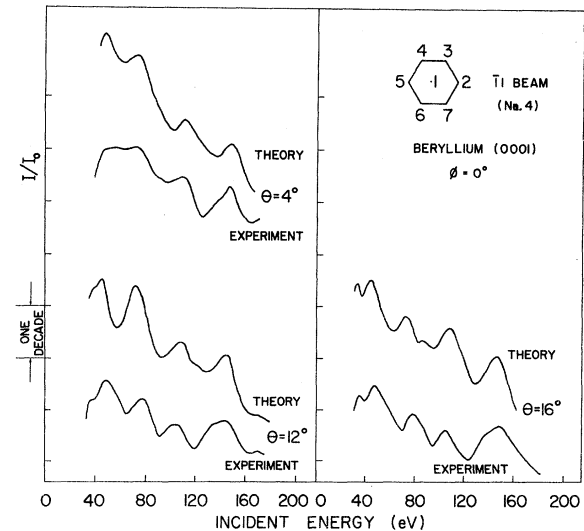


FIG. 8. Direct comparison between experimental and calculated  $\bar{1}1$  spectra for  $\phi = 0^\circ$ , and  $\theta = 4^\circ, 12^\circ$ , and  $16^\circ$ .



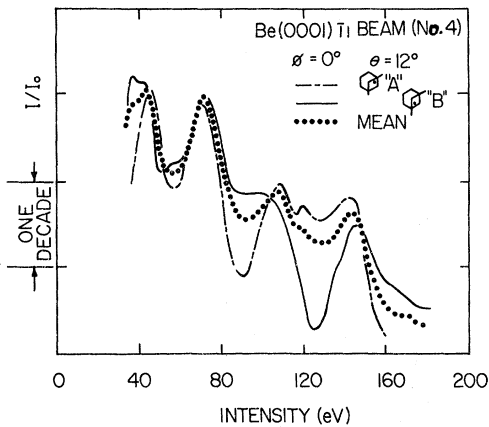


FIG. 9. Calculated  $\bar{1}1$  spectra for  $\theta = 12^\circ$  and  $\phi = 0^\circ$ . The solid curve represents the spectrum from a surface that terminates in the *B* configuration as shown in Fig. 10. The broken curve represents the spectrum from a surface that terminates in the *A* configuration as shown in Fig. 10. The dotted curve is the average of the two other curves.

For  $l = 3, 7, 11$ , the quantities  $C_{n,m}$  have the opposite sign. The even values of  $l$  give rise to zero differences according to point (b). Thus we see that the different terminations may give different results for the intensities of the nonspecular beams. In particular, for a nonspecular beam for which  $2n + m$  is not a multiple of three, kinematic theory yields a difference which is zero at a Bragg reflection and increases to a maximum halfway between Bragg reflections, alternating in sign between successive Bragg reflections. In Fig. 9, the effect of termination on the  $\bar{1}1$  beam for  $\theta = 12^\circ$  and  $\phi = 0^\circ$  is shown by means of a plot of the intensities (calculated with the method described in Ref. 19) relative to each termination. If the electron beam illuminates a region containing a large number of atomic steps equally distributed over the two terminations, an average spectrum will result. As this situation is most probable in the experiments described above, we have averaged the intensities calculated for the two terminations and have plotted the averaged curve in Fig. 9 as well. The curves presented in the Figs. 2(b) and 3(b) are all averages of curves calculated for the two terminations *A* and *B*.

It is interesting to consider whether these results are applicable to reflections from the  $\{111\}$  surface of a face-centered-cubic crystal. This surface is also close-packed but differs from its hexagonal counterpart in the stacking sequence along the  $\langle 111 \rangle$  direction. The stacking sequence is of course *ABCABC...* instead of *ABABAB...*. If the absorption is so large that only the first two layers are effectively probed by the electron beam, then one might suspect that both the fcc  $\{111\}$  and

the hcp (0001) surfaces should be treated alike, i. e., that different terminations would produce different LEED spectra from fcc  $\{111\}$  surfaces as well. This is not the case since the relationship between the first and second layers of an fcc  $\{111\}$  surface is determined *only* by the orientation of the crystal and *not* by which layer terminates the crystal. Inspection of the fcc lattice shows that the *A* plane bears the same relationship to the *B* plane as *B* does to *C*, i. e., the *C* plane can be obtained from *B* with the same translation that produces *B* from *A*. For hexagonal-close-packed crystals, however, the relationship (see Fig. 10) is determined by terminations, because the displacement that produces the *B* plane from the *A* plane is opposite in sign to that which produces the *A* from the *B* plane. In other words, the face centered cubic is a *Bravais* lattice with one atom per unit cell and thus all structure factors have unit magnitude. This is not so for the hexagonal-close-packed structure.

In conclusion we emphasize two points. First,

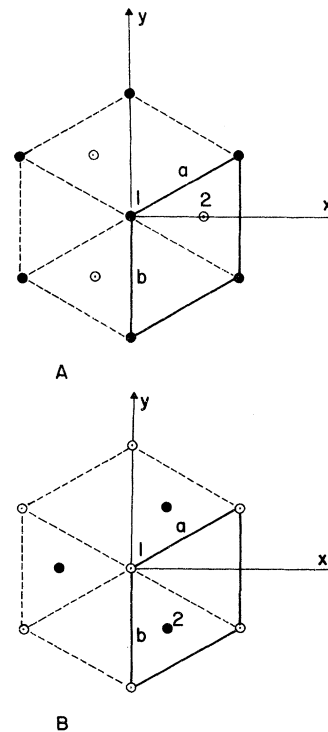


FIG. 10. Schematic drawing, in real space, of the basal plane of the hexagonal-close-packed structure. The top figure depicts the *A* termination: the open circles represent the top layer, the full circles the second layer. The bottom figure depicts the *B* termination: The solid circles represent the top layer, the open circles the second layer. The unit mesh is defined by the vectors  $\vec{a}$  and  $\vec{b}$  (given in the text). The two atoms in the unit cell are labeled 1 and 2.

the calculated results for the nonspecular beams from Be(0001) are in reasonable agreement with the experimental data. This lends encouragement towards the goal of calculation of LEED intensities both accurately and rapidly so that LEED data can be useful in surface-structure determination. Secondly, non-Bravais-lattice crystal structures can give rise to diffraction features in the non-

specular beams which are dependent on the termination plane and hence indirectly on the distribution of steps. If there are many steps illuminated by the beam, the resulting intensities are averages over the various diffractions from each type of surface exposed. If there are few or no steps the diffracted intensities are specific to the termination exposed.

\*The work of these authors was sponsored in part by the Air Force Office of Scientific Research, Air Force Systems Command, under Grant No. AFOSR-69-1707.

<sup>1</sup>J. L. Beeby, *J. Phys. C* **1**, 82 (1968).

<sup>2</sup>D. S. Boudreaux and V. Heine, *Surface Sci.* **8**, 426 (1967).

<sup>3</sup>G. Capart, *Surface Sci.* **13**, 361 (1969).

<sup>4</sup>C. B. Duke and C. W. Tucker, Jr., *Phys. Rev. Letters* **23**, 1163 (1969).

<sup>5</sup>C. B. Duke, A. J. Howsmon, and G. E. Laramore, *J. Vac. Sci. Technol.* **8**, 10 (1971).

<sup>6</sup>K. Hirabayashi and Y. Takeishi, *Surface Sci.* **4**, 150 (1966).

<sup>7</sup>V. Hoffstein and D. S. Boudreaux, *Phys. Rev. Letters* **25**, 512 (1970).

<sup>8</sup>P. J. Jennings and E. G. McRae, *Surface Sci.* **23**, 363 (1970).

<sup>9</sup>D. W. Jepsen, P. M. Marcus, and F. Jona, *Phys. Rev. Letters* **26**, 1365 (1971); *Phys. Rev. B* **5**, 3933 (1972).

<sup>10</sup>R. O. Jones and J. A. Strozier, Jr., *Phys. Rev. Letters* **22**, 1186 (1969).

<sup>11</sup>K. Kambe, *Z. Naturforsch.* **22a**, 322 (1967); **22a**, 422 (1967).

<sup>12</sup>G. E. Laramore, C. B. Duke, A. Bagchi, and A. B. Kunz, *Phys. Rev. B* **4**, 2058 (1971).

<sup>13</sup>G. E. Laramore and C. B. Duke, *Phys. Rev. B* **5**, 267 (1972).

<sup>14</sup>P. M. Marcus and D. W. Jepsen, *Phys. Rev. Letters* **20**, 925 (1968).

<sup>15</sup>E. G. McRae and P. J. Jennings, *Surface Sci.* **15**, 345 (1969).

<sup>16</sup>E. G. McRae and D. E. Winkel, *Surface Sci.* **14**, 407 (1969).

<sup>17</sup>Y. H. Ohtsuki, *J. Phys. Soc. Japan* **24**, 1116 (1968); **25**, 481 (1968).

<sup>18</sup>J. B. Pendry, *J. Phys. C* **1**, 1065 (1968); **2**, 1215 (1969); *Phys. Rev. Letters* **27**, 856 (1971).

<sup>19</sup>J. A. Strozier and R. O. Jones, *Phys. Rev. Letters* **25**, 516 (1970); *Phys. Rev. B* **3**, 3228 (1971).

<sup>20</sup>S. Y. Tong and T. N. Rhodin, *Phys. Rev. Letters* **26**, 711 (1971).

<sup>21</sup>C. M. K. Watts, *J. Phys. C* **1**, 1237 (1968); **2**, 966 (1969).

<sup>22</sup>F. Jona, *IBM J. Res. Develop.* **14**, 444 (1970).

<sup>23</sup>M. G. Lagally, *Z. Naturforsch.* **25a**, 1567 (1970).

<sup>23a</sup>M. P. Seah, *Surface Sci.* **17**, 181 (1969).

<sup>24</sup>D. W. Jepsen, P. M. Marcus, and F. Jona, in Fifth LEED Seminar, National Bureau of Standards, Washington, D. C. (unpublished).

<sup>25</sup>S. Andersson, *Surface Sci.* **18**, 325 (1969).

<sup>26</sup>L. R. Bedell, thesis (Brown University, 1970) (unpublished).

<sup>27</sup>J. A. Strozier, Jr., R. O. Jones, and F. P. Jona, in Ref. 24.

<sup>28</sup>J. M. Baker and J. M. Blakely (unpublished); for details, see J. M. Baker, thesis (Cornell University, 1970) (unpublished).

<sup>29</sup>F. Jona and H. R. Wendt, *Rev. Sci. Instr.* **40**, 1172 (1969).

<sup>30</sup>Varian Associates, Palo Alto, Calif.

<sup>31</sup>R. O. Adams, *Mater. Res. Bull.* **2**, 469 (1967); see also, *The Structure and Chemistry of Solid Surfaces*, edited by G. A. Somorjai (Wiley, New York, 1968), pp. 70-71.

<sup>32</sup>Ultra-Sensitive Brightness Spot Meter, Photo Research Corp., Hollywood, Calif.

<sup>33</sup>We are very grateful to Dr. Baker and Prof. Blakely for providing us with their large original recorder charts. Since their energy scale was identical to ours (20 eV/in.) we were in a position to compare any two spectra by laying one directly over the other.

<sup>34</sup>M. G. Lagally, T. C. Ngoc, and M. B. Webb, *Surface Sci.* **2**, 444 (1971).

<sup>35</sup>See any text on kinematic theory of diffraction.